THE ASTROPHYSICAL JOURNAL, 411:794–796, 1993 July 10

3.3 AND 11.3 MICRON IMAGES OF HD 44179: EVIDENCE FOR AN OPTICALLY THICK POLYCYCLIC AROMATIC HYDROCARBON DISK

JESSE D. BREGMAN,[1] DAVID RANK,[2] PASQUALE TEMI,[2] DOUG HUDGINS,[1] AND LAURA KAY[1,3]
Received 1992 October 15; accepted 1993 January 5

ABSTRACT

Images of HD 44179 (the Red Rectangle) obtained in the 3.3 and 11.3 μm emission bands show two different spatial distributions. The 3.3 μm band image is centrally peaked and slightly extended N-S while the 11.3 μm image shows a N-S bipolar shape with no central peak. If the 3.3 μm band image shows the intrinsic emission of the 11.3 μm band, then the data suggest absorption of the 11.3 μm emission near the center of HD 44179 by a disk with an optical depth of about 1, making HD 44179 the first object in which the infrared emission bands have been observed to be optically thick. Since there is no evidence of absorption of the 3.3 μm emission band by the disk, the absorption cross section of the 3.3 μm band must be substantially less than for the 11.3 μm band. Since the 3.3 and 11.3 μm bands are thought to arise from different size PAHs, the similar N-S extents of the two images implies that the ratio of small to large PAHs does not change substantially with distance from the center.

Subject headings: infrared: interstellar: continuum — ISM: individual (Red Rectangle) — ISM: molecules — stars: individual (HD 44179)

1. INTRODUCTION

HD 44179 (the "Red Rectangle") is a strong infrared source (AFGL 915) consisting of a pair of A0 stars and a bipolar nebula (Cohen et al. 1975). The bipolar structure presumably is created by mass loss from the central stars directed by a disk. Dainty et al. (1985) observed that the *K* and *L* band emission was extended 1.″05 N-S by 0.″4 E-W. The infrared spectrum of HD 44179 shows both a smooth continuum which is much broader than a blackbody and the infrared emission bands associated with carbonaceous material (Cohen et al. 1975; Russell, Soifer, & Willner 1978). The suggested identification of the carbonaceous material includes polycyclic aromatic hydrocarbon (PAH) molecules and PAH clusters (Leger & Puget 1984; Allamandola, Tielens, & Barker 1985), hydrogenated amorphous carbon (HAC) particles (Duley & Williams 1981), and quenched carbonaceous composite (QCC) particles (Sakata et al. 1984). All of these materials contain only carbon and hydrogen atoms, and contain or are dominated by aromatic (sp^2) carbon skeletons (Robertson & O'Reilly 1987).

A set of weaker bands longward of the strong 3.3 μm band has been attributed to emission from an excited state from PAHs and combination/overtone modes (Allamandola et al. 1985; Sandford 1991), to $-CH_2$ or $-CH_3$ sidegroups (Duley & Williams 1981; de Muizon et al. 1986; Jourdain de Muizon, d'Hendecourt, & Geballe 1990; Nagata et al. 1988), and to PAHs with extra hydrogen atoms connected to the carbon atoms in their rings (M. de Groot 1992, private communication; Schutte, Tielens, & Allamandola 1993). Geballe et al. (1989) had observed the 3.2–3.6 μm region both centered on HD 44179 and 5″ north of the star. While the overall emission was much weaker north of the star, the ratio of the 3.4 to 3.3 μm bands increased, perhaps indicating that smaller PAHs were completely dehydrogenated in the intense UV field near the center. Bregman et al. (1993) showed that the relative distribution of the 3.3 and 11.3 μm emission bands in NGC 1333 was consistent with dehydrogenation of small PAHs close to the exciting star SVS 3.

HD 44179 should provide an interesting comparison with NGC 1333 and another test of the suggestion that dehydrogenation of PAHs can explain the relative distributions of the 3.3 and 11.3 μm emission features. The exciting stars in HD 44179 are more luminous that SVS 3 but are also cooler. Most of the emission from HD 44179 occurs closer to the exciting source than in NGC 1333, so the intensity of the UV field is greater in the emitting region in HD 44179. Dehydrogenation of small PAHs should be greater in the center of HD 44179 than in NGC 1333. From these arguments and the observations by Geballe et al. (1989), we would expect that farther from the exciting stars, small PAHs would be more abundant relative to large PAHs.

2. OBSERVATIONS AND INSTRUMENT DESCRIPTION

The observations were made from the NASA/University of Arizona 1.5 m telescope on Mount Lemmon in 1991 November. Two infrared cameras were used, one with a 128 × 128 InSb array and the other with a 128 × 128 Si:Ga array. Both arrays were manufactured by Amber Engineering. The cameras use similar LHe Dewars so that either an InSb or Si:Ga array can be used with common controller and data acquisition electronics. The Si:Ga array requires LHe operation while the InSb detector was operated at pumped LN_2 temperatures. Antireflection coated lens, filter, and widow assemblies are optimized for the band pass of the two different arrays. Each camera has a filter wheel, a 38 mm f/1.5 ZnSe reimaging lens (operating at a focal reduction of 2), with field and Lyot stop baffles. The InSb camera has six fixed filters and the Si:Ga camera has four fixed filters and a 1.8% spectral resolution 8–14 μm CVF. The InSb camera has an image scale of 0.″75 per pixel and the Si:Ga camera has an image scale of 0.″96 per pixel on the 1.5 m telescope. The images of HD 44179

[1] MS245-6, NASA Ames Research Center, Moffett Field, CA 94035-1000.
[2] UCO and Lick Observatory, UCSC, Santa Cruz, CA 95064.
[3] Barnard College, Physics Department, 3009 Broadway, New York, NY 10027.

were obtained by chopping the source 90″ N-S at a frequency of 1 Hz. Frames were co-added for 30–60 s, then the telescope was nodded to allow cancellation of telescope background and offset. An optical CCD guide camera and a gold coated dichroic beam splitter were used, allowing for accurate guiding with a computer controlled autoguider. The autoguider reduces image motion to a fraction of an arcsecond, and insures that the image is returned to the same place on the infrared array during nodding of the telescope.

To isolate the 3.3 and 11.3 μm emission features from the underlying continuum, images obtained at wavelengths centered on the bands were subtracted from images obtained at nearby wavelengths. For the 3.3 μm band, a 0.062 μm wide filter centered at 3.1 μm was used to measure the continuum while a 0.12 μm wide filter centered at 3.3 μm was used to measure the emission band. The relative transmissions through the filters was measured by observing the star Beta Gem. The image of the 3.3 μm feature is then the difference of the images obtained through the two filters with corrections made for instrumental and atmospheric transmission differences, and for the relative continuum intensities observed by Russell, Soifer, & Merrill (1977) between 3.1 and 3.3 μm. The 11.3 μm emission band image is the difference of two images obtained through a 2% spectral bandwidth CVF, one centered on the 11.3 μm band and the other at 10.5 μm. Instrumental and atmospheric transmission corrections were measured by observing Alpha Tau at both wavelengths, and the observations by Witteborn et al. (1989) were used to correct for the continuum slope between 10.5 and 11.3 μm. We found that the total corrections were a factor of 3.18 for the 3.1 μm image relative to the 3.3 μm image and a factor of 1.06 for the 10.5 μm image relative to the 11.3 μm image.

The results are shown in Figure 1 (Plate 6) as a combination of the 3.3 and 11.3 μm emission feature images of HD 44179. The 3.3 μm data is shown in contour intervals of 400 mJy arcsec^{-2}, with the lowest contour at 320 mJy arcsec^{-2}. The 11.3 μm image is displayed in color with blue indicating low brightness and red indicating high brightness, with a peak intensity of 1.4 Jy arcsec^{-2}. The images were registered using the bright central star. Rotation of each of the two cameras was measured by trailing a star N-S across the array while taking a long integration. The measured rotation relative to the N-S direction was 0° for the InSb camera and 3°.5 west of north (clockwise) for the Si:Ga camera. The 11.3 μm image was rotated 3°.5 counterclockwise before registration with the 3.3 μm image.

3. DISCUSSION

The distribution of the 11.3 μm emission band is similar to the optical emission from the nebula, showing a bipolar distribution with sharp edges. The optical data have been explained as a bicone of material directed by a central disk (Cohen et al. 1975). The 3.3 μm image is quite different, showing a centrally bright distribution with some north-south extension. If the intrinsic emission distribution from the two bands is the same, then a comparison of these two images implies that the 11.3 μm emission suffers from self-absorption by a horizontal disk with an optical depth in the 11.3 μm band of about 1. Also, the 3.3 μm band shows no evidence for self-absorption, and thus must have a small optical depth through the disk. This has implications for the relative absorption cross sections of the two bands. Leger, d'Hendecourt, & Defourneau (1989) estimate a cross section for the 11.3 μm band which is 9 times greater than for the 3.3 μm band based on laboratory absorption spectra of small PAHs. Schutte et al. estimate a cross section of the 11.3 μm band which is 8.6 times larger than for the 3.3 μm band based on laboratory gas phase measurements. If our explanation for the data presented here is correct, then the absorption cross section of the 11.3 μm band must be significantly more than for the 3.3 μm band, in good agreement with the laboratory data for PAHs. HD 44179 is the first object which appears to be optically thick in any of the infrared emission bands. Also, assumptions that the presence of the infrared emission bands implies optically thin emission (e.g., Dainty et al. 1985) applies only to the continuum, not to the emission bands themselves.

The 11.3 μm band emission and optical depth can be examined in several ways. Observationally, Witteborn et al. (1989) showed that the 11.3 μm emission band in HD 44179 was broader than that of three other objects and it had a flat top, consistent with a self-absorbed feature. Using the values given by Schutte et al. (1992) for the 11.3 μm band of 2.5×10^{-19} cm^2 per C-H bond, we find an optical depth of 1 requires a column density of PAH C-H bonds of 4×10^{18} cm^{-2}. Since HD 44179 is carbon-rich, the ratio of C/H atoms should be greater than cosmic, so we will use $N_C/N_H = 3 \times$ cosmic $= 1 \times 10^{-3}$. If 10% of the carbon is in the form of PAHs and the number of C-H bonds is a third of the number of carbon atoms, then the total column density is 1×10^{23} cm^{-2}. Using a distance to HD 44179 of 330 pc (Cohen et al. 1975), and assuming the disk is confined to the central 1″, the average density of the disk would be about 2×10^7 cm^{-3}, not entirely unreasonable for a thick disk.

The measured continuum emission in the mid-infrared wavelengths can provide a second method of estimating the optical depth through the disk in the 11.3 μm band. Dainty et al. (1985) argue that the dust temperature 0″.5 from the central star is consistent with the 10 μm color temperature of 500 K. Using this value for the dust temperature and the size for the emitting region measured by Dainty et al. (1985) of 0″.4 × 1″.05, the continuum optical depth at 10.5 μm is 0.013. Cohen et al. (1975) concluded that the dominant dust particle radius was about 1 μm. Such large grains will be nearly optically thick at 10 μm, thus the optical depth of 0.013 can be viewed as a filling factor (i.e., 1.3% of the field of view is filled with 1 μm radius dust grains). Each grain has an area of 3×10^{-8} cm^2, so the total number of grains along the line of sight is 4×10^5 cm^{-2}, and the corresponding dust mass (using the density of graphite of 2.26 gm cm^{-3}) is 4×10^{-6} cm^{-2}. Tielens (1989) showed that the number of PAHs fit the standard Mathis, Rumpl, & Nordsieck (1977) power law appropriate for graphitic dust particles (i.e., $N \propto a^{-3.5}$, or $M \propto a^{-0.5}$). A 100 C atom condensed PAH (e.g., $C_{94}H_{26}$) has a radius of $\approx$5 Å. Using the above mass versus size relationship, there should be 45 times as much mass in large PAHs as in 1 μm radius carbon dust, which corresponds to 9×10^{18} C atoms in large PAHs. The number of C-H bonds in a 100 C atom PAH is about a third of the number of C atoms. So, using the absorption cross section for the 11.3 μm band of 2.5×10^{19} cm^2 (Schutte et al. 1993), the optical depth from PAHs is then $\approx$0.8, comparable to the value calculated from the 11.3 μm image assuming the central disk was absorbing at 11.3 μm. Even though the assumptions used in this line of reasoning are plausible, there are many uncertainties in this calculation. The calculation is used to show that an optical depth of about 1 in the 11.3 μm PAH band is consistent with other observations of HD 44179.

The relative spatial extents of the 3.3 and 11.3 μm emission bands has some implications for the suggestion that the 3.4 μm emission band is due to an excited state transition in small PAHs. Geballe et al. (1989) had observed that at a position 5″ north of the center, the 3.4 μm band was stronger relative to the 3.3 μm band than at the center position. For the same excitation energy, small PAHs have a larger 3.4/3.3 μm band radio than do large PAHs. Also, small PAHs are more easily dehydrogenated than large PAHs. Thus, they suggested that dehydrogenation of small PAHs close to the center could account for the band ratios, and the relative amount of small to large PAHs increases with distance from the center. This effect might be observable in the relative distributions of the 3.3 and 11.3 μm emission bands since small PAHs also have a larger 3.3/11.3 μm band ratio than large PAHs. If the ratio of small to large PAHs increases significantly with distance from the center, we might expect the image of the 3.3 μm emission band to have a greater N-S extent than the 11.3 μm image. However, the data show that the 3.3 and 11.3 μm emission images have about the same extent and shape at their north and south extremes, with the 11.3 μm image being slightly more extended. Thus, for HD 44179, these data support one of the other origins for the 3.4 μm band (i.e., $-CH_2$ or $-CH_3$ side groups or multiple hydrogen atoms per C atom as in cyclo-hexane).

4. CONCLUSIONS

Images of HD 44179 (the Red Rectangle) obtained in the 3.3 and 11.3 μm emission bands show two different spatial distributions. The 3.3 μm band image is centrally peaked and slightly extended N-S, while the 11.3 μm image shows a N-S bipolar shape with no central peak. If the 3.3 μm band image shows the intrinsic emission of the 11.3 μm band, then the data can be explained as self-absorption of the 11.3 μm emission near the center of HD 44179 by a disk with an optical depth of about 1. The absorption cross section of the 3.3 μm band must be substantially less than for the 11.3 μm band, in agreement with the laboratory values for PAHs. The similar N-S extents of the two images implies that the ratio of small to large PAHs does not change substantially with distance from the center. Finally, we point out that the assumption that the presence of the infrared emission bands implies that the emission is optically thin (e.g., Dainty et al. 1985) applies only to the continuum emission and not the emission bands themselves.

We wish to thank Scott Sandford for helping with the observations, and Fred Witteborn for helping with the equipment. The Mount Lemmon observatory staff provided valuable assistance in setting up the equipment and preparing the telescope for operation.

REFERENCES

Allamandola, L. J., Tielens, A. G. G. M., & Barker, J. R. 1985, ApJ, 290, L25
Bregman, J., Rank, D., Sandford, S. A., & Temi, P. 1993, ApJ, 410, 668
Cohen, M. et al. 1975, ApJ, 196, 179
Dainty, J. C., Pipher, J. L., Lacasse, M. G., & Ridgway, S. T. 1985, ApJ, 293, 530
de Muizon, M., Geballe, T. R., d'Hendecourt, L. B., & Bass, F. 1986, ApJ, 306, L105
Duley, W. W., & Williams, D. A. 1981, MNRAS, 196, 269
Geballe, T. R., Tielens, A. G. G. M., & Allamandola, L. J., Moorhouse, A., & Brand, P. W. J. L. 1989, ApJ, 341, 278
Jourdain de Muizon, M., d'Hendecourt, L. B., & Geballe, T. R. 1990, A&A, 235, 367
Leger, A., d'Hendecourt, L. B., & Defourneau, D. 1989, A&A, 216, 148
Leger, A., & Puget, J. L. 1984, A&A, 137, L5
Mathis, J. S., Rumpl, W., & Nordsieck, K. H. 1977, ApJ, 217, 425
Nagata, T., Tokunaga, A. T., Sellgren, K., Smith, R. G., Onaka, T., Nakada, Y., & Sakata, A. 1988, ApJ, 326, 157
Robertson, J., & O'Reilly, E. P. 1987, Phys. Rev. B, 35, 2946
Russell, R. W., Soifer, B. T., & Merrill, K. M. 1977, ApJ, 213, 66
Russell, R. W., Soifer, B. T., & Willner, S. P. 1978, ApJ, 220, 568
Sakata, A., Wada, S., Tanabe, T., & Onaka, T. 1984, ApJ, 287, L51
Sandford, S. A. 1991, ApJ, 376, 599
Schutte, W. A., Tielens, A. G. M., & Allamandola, L. J. 1993, ApJ, in press
Tielens, A. G. G. M. 1989, in Interstellar Dust, L. J. Allamandola & A. G. G. M. Tielens (Dordrecht: Kluwer), 239
Witteborn, F. C., Sandford, S. A., Bregman, J. D., Allamandola, L. J., Cohen, M., Wooden, D. H., & Graps, A. L. 1989, ApJ, 341, 270

PLATE 6

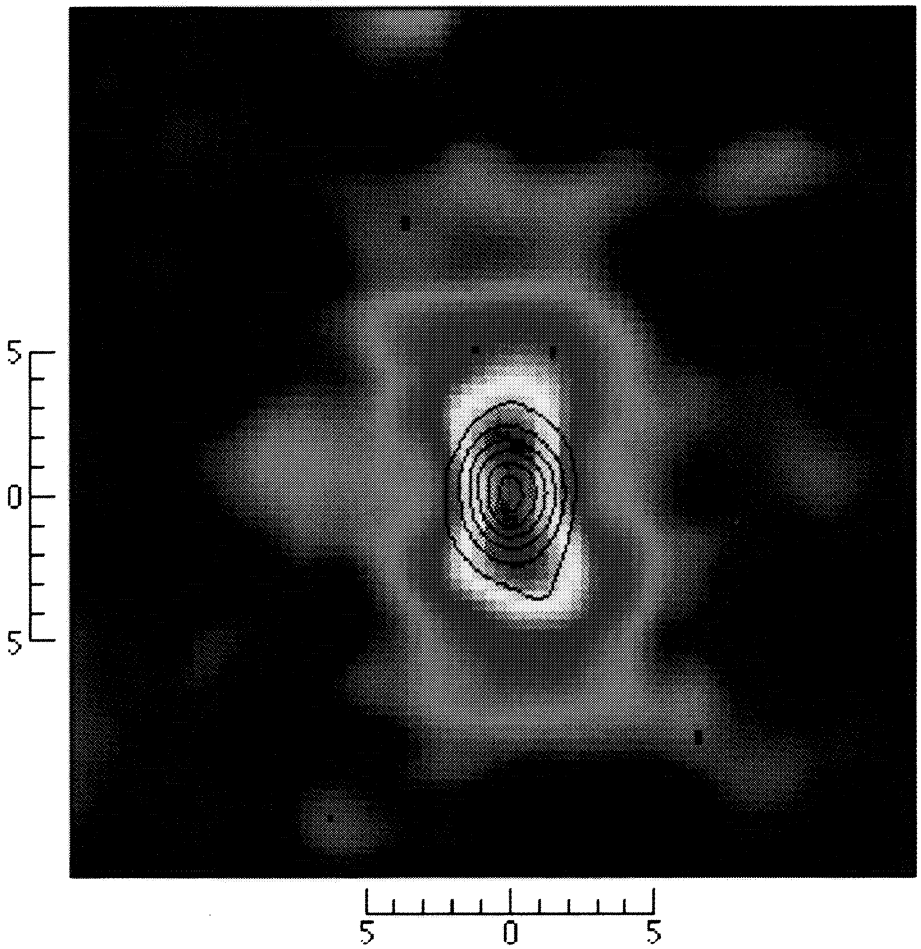

FIG. 1.—11.3 μm emission in HD 44179 is shown in color, with red indicating the maximum brightness (1.4 Jy arcsec^{-2}) and blue the minimum brightness. The contours show the distribution of 3.3 μm emission. The lowest 3.3 μm contour is 320 mJy arcsec^{-2} and the contours are spaced at equal intervals of 400 mJy arcsec^{-2}. North is up and east is to the left. The scales are in arcseconds.

BREGMAN et al. (see 411, 795)